

Bridge the Cosmological Tensions with Thawing Gravity

Gen Ye*

Institute Lorentz, Leiden University,

PO Box 9506, Leiden 2300 RA, The Netherlands

Abstract

It is found that a non-minimally coupled scalar tensor theory, Thawing Gravity (TG), can explain multiple tensions plaguing the standard cosmological model Λ CDM while fitting better to observations than the latter. Using the standard Bayes model comparison method, TG has moderate evidence over Λ CDM with a Bayes factor $\ln B = +1.5$ in the baseline analysis including CMB, BAO and SNIa. In the baseline+ H_0 analysis which further takes into account the Cepheids calibration of the SNIa distance ladder from SH0ES, TG has very strong evidence over Λ CDM with $\ln B = +11.8$. In particular, TG yields $H_0 = 71.78 \pm 0.86$ km/s/Mpc and $S_8 = 0.793 \pm 0.012$, consistent with both local H_0 measurement and the large scale structure surveys.

arXiv:2411.11743v1 [astro-ph.CO] 18 Nov 2024

* ye@lorentz.leidenuniv.nl

I. INTRODUCTION

The past two decades have seen great success of the standard model of cosmology, the cosmological constant cold dark matter model (Λ CDM), which provides satisfying description to most cosmological observations with only six parameters. Nevertheless, studies in recent years center around the cosmological tensions, inconsistencies with various significance between Λ CDM and recent observations [1–3].

Most significantly, there is the Hubble tension [4, 5] where the locally measured expansion rate of the Universe, $H_0 = 73.04 \pm 1.04$ km/s/Mpc $^{-1}$ reported by the SH0ES group [6], is in $> 5\sigma$ tension with that, e.g. $H_0 = 67.66 \pm 0.42$ km/s/Mpc $^{-1}$ by Planck [7], derived from the Λ CDM model calibrated by the cosmic microwave background (CMB) and baryon acoustic oscillations (BAO), two of the most robust cosmological observations.

There is also the so-called S_8 tension [8], in which the parameter $S_8 = \sigma_8 \sqrt{\Omega_m/0.3}$ measured by the galaxy weak lensing surveys is usually $2 - 3\sigma$ lower than that derived from CMB and BAO calibrated Λ CDM. σ_8 is the standard deviation of linear matter density fluctuation in a sphere with radius $8 h^{-1}$ Mpc, and the matter fraction Ω_m is included in the definition to account for inherent cosmic shear degeneracy. The S_8 tension is far less significant than the Hubble tension, in particular the most recent measurement from DESY3 and KiDS reduces it from a tension to a marginal agreement at 1.7σ with the Planck result based on CMB calibrated Λ CDM [9].

More recently, DESI reported a new inconsistency with Λ CDM in its first year BAO measurement [10]. When further combined with CMB and type Ia supernovae (SNIa) distance ladder observations from either Pantheon+ [11], Union [12] or DES Y5 [13], this yields preference for dynamical dark energy (DE) over a cosmological constant Λ at 2.5σ , 3.5σ or 3.9σ respectively [10]. Whether it is driven by systematics or not is still under discussion [14–26]. Even without SNIa, it is still important that the new DESI results, for the first time in the past two decades, reveals inconsistency in Λ CDM between CMB and BAO, which probe with great precision the same sound horizon scale at times separated by billions of years, thus forming one of the most stringent consistency tests of the cosmological model.

Ye *et al.* [27] suggests that, if the DESI and SNIa finding is not significantly biased by systematics, these observations further indicate phantom crossing in DE at $z < 1$, and signal modified gravity (MG), especially non-minimal coupling between gravity and matter,

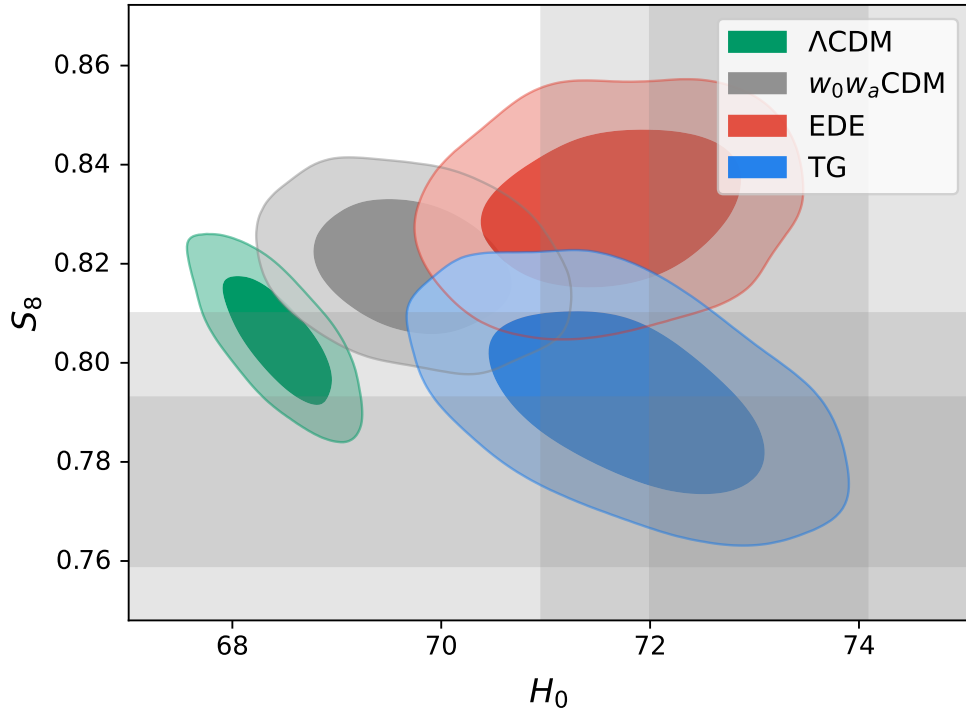


FIG. 1. 68% and 95% posterior distributions of H_0 and S_8 for all models in the baseline+ H_0 analysis. Gray bands mark the 1σ and 2σ region of the locally measured H_0 [6] and S_8 [9].

on cosmological scales. Based on these insights, Ye *et al.* [27] suggested a covariant effective field theory (EFT) of gravity on cosmological scales, dubbed *Thawing Gravity* (TG),

$$\mathcal{S} = \int dx^4 \sqrt{-g} \left[\frac{M_p^2}{2} f(\phi) R + X - V(\phi) \right] + \mathcal{S}_m[g_{\mu\nu}] \quad (1)$$

where $X \equiv -\frac{1}{2}g^{\mu\nu}\nabla_\mu\phi\nabla_\nu\phi$ and the reduced Planck mass $M_p^2 = (8\pi G_N)^{-1}$, G_N being the Newtonian constant today. $V(\phi)$ is assumed to be the DE potential that supports accelerated expansion. There is no strong constraint from observation on the form of the DE potential $V(\phi)$. Recently it is suggested that using a hill-top form for $V(\phi)$ might be preferable [28]. Though originally proposed to explain the DESI finding, this paper studies TG as a full cosmological model and confronts it with state-of-the-art observations of CMB, BAO, SNIa as well as large scale structure (LSS) and local measurement of H_0 . The results indicate that TG is a promising cosmological model that naturally addresses the major cosmological tensions, see Fig.1. Based on the Jeffreys scale [29], with CMB, BAO and SNIa alone, TG yields moderate evidence over Λ CDM with a Bayes factor $\ln B = +1.5$. The evidence of TG over Λ CDM becomes very strong with $\ln B = +11.8$ when the SH0ES calibration of

SN Ia is included, because TG also resolves the Hubble tension. At early times, TG behaves effectively as early dark energy (EDE) [30, 31], see also e.g. [32–35] and [36, 37] for recent reviews of EDE, but does not suffer from the coincidence problem of EDE (i.e. “why does the EDE contribution become significant precisely close to matter-radiation equality”) nor the exacerbated S_8 tension [38], because the TG field is naturally triggered at matter-radiation equality when the background Ricci curvature becomes comparable to the Hubble energy scale and the associated MG effect cures the enhancement in S_8 . As a result, TG also yields moderate evidence over EDE with a Bayes factor $\ln B = +2.3$.

Section II describes the theoretical aspects of TG, with screening discussed in Appendix A. The data analysis setup and methods are described in Section III. The key results are presented and discussed in Section IV, with large plots and tables collected in Appendix B. Section V provides a short summary.

II. THAWING GRAVITY

The corresponding Einstein and scalar field equations of TG (1) are

$$fG_{\mu\nu} + \square f g_{\mu\nu} - \nabla_\mu \nabla_\nu f = \frac{1}{M_p^2} [T_{\mu\nu}^{(\phi)} + T_{\mu\nu}^{(m)}], \quad (2)$$

$$-\square\phi = \frac{M_p^2}{2} f' R - V' \quad (3)$$

where $T_{\mu\nu}^{(\phi)} = \phi_\mu \phi_\nu + g_{\mu\nu} [X - V]$ and $T^{(m)}$ is the stress energy tensor for the matter. The scalar field has an effective potential

$$V_{\text{eff}} = \frac{M_p^2}{2} R f(\phi) - V(\phi). \quad (4)$$

Following Ye *et al.* [27] I adopt the exponential potential $V = V_0 \exp(-\lambda\phi/M_p)$ typical for DE ¹, and the non-minimal coupling function $f(\phi) = 1 - \xi(\phi/M_p)^2$, which captures the common structure around a local minima of a general $f(\phi)$. An interesting feature of such forms of non-minimal coupling is the existence of a GR attractor, which appears if $f(\phi)$ has a local minimum and R dominates over V in the early times (still in matter domination) [27, 39].

¹ Ref.[28] reported that a hill-top potential might provide a better fit to data than an exponential one when more than half of the numerical analysis in this paper has already completed. Using the new potential will only further strengthen the conclusions of this paper.

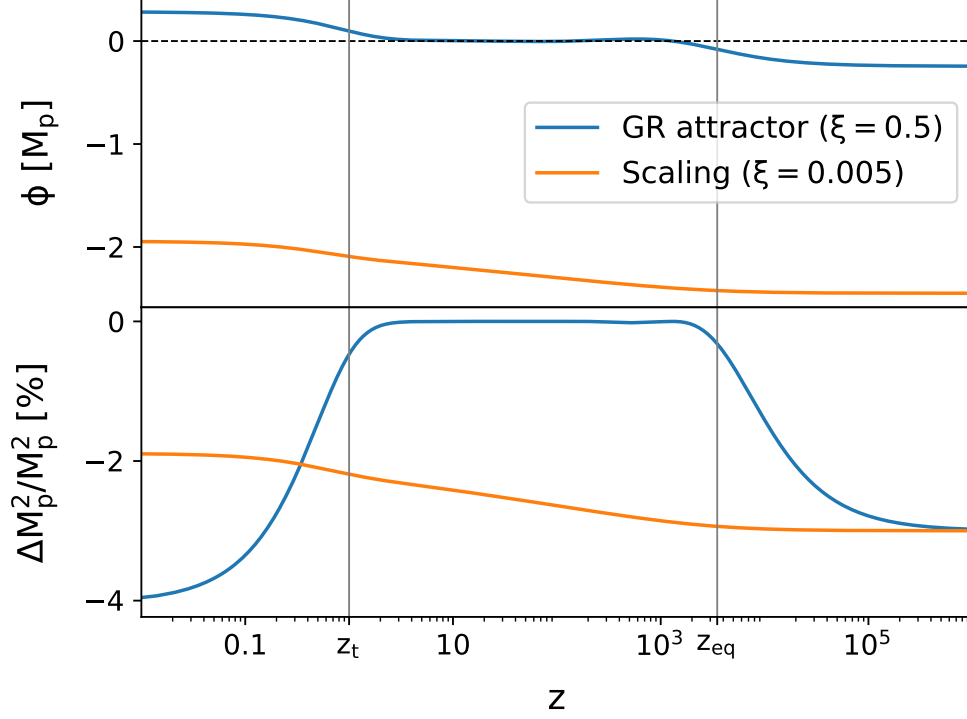


FIG. 2. Evolution of the scalar field and runing of the Planck mass $\Delta M_p^2/M_p^2 \equiv M_{\text{eff}}^2/M_p^2 - 1 = -\xi(\phi/M_p)^2$ in the GR attractor and scaling solutions. The vertical gray lines mark the approximate position of thawing $z_t \simeq 1$ and the matter-radiation equality $z_{\text{eq}} \simeq 3500$.

In an FRW background, Eqs.(2) and (3) simplify to

$$3M_p^2 H^2 [1 - \xi(\phi/M_p)^2] - 18\xi\phi\dot{\phi}H = \frac{1}{2}\dot{\phi}^2 + V(\phi) + \rho_m, \quad (5)$$

$$\ddot{\phi} + 3H\dot{\phi} + V_\phi + 6\left(2 + \frac{\dot{H}}{H^2}\right)\xi H^2\phi = 0. \quad (6)$$

Since $V(\phi)$ is the DE potential, in both the radiation dominant (RD) and matter dominant (MD) eras one has $V/H^2 \ll 1, V_\phi/H^2 \ll 1$. Therefore one can neglect $V(\phi)$ and obtain the following approximate solution in RD and MD respectively

$$\phi \simeq \begin{cases} \phi_{\text{ini}} & \text{RD,} \\ \phi_{\text{ini}} \exp\left[\frac{-3 \pm \sqrt{9 - 48\xi}}{4}(N - N_i)\right] & \text{MD,} \end{cases} \quad (7)$$

where $N = \ln a/a_0$ is the e-folding number. According to Eq.7, the field stays nearly constant during RD. Physically, this is because $R \ll H^2$ in RD and the field is frozen by the Hubble friction. It begins to roll when the Universe switches to MD near matter-radiation equality

and $R \sim \mathcal{O}(H^2)$. At this time TG effectively acts as an EDE component and reduces the sound horizon near recombination, resulting in a larger Hubble constant compatible with local measurements. Therefore TG provides a natural explanation of the Hubble tension but does not suffer from the coincidence problem plaguing the the EDE theories. The evolution of TG after recombination falls into two categories depending on the value of ξ :

- **GR attractor** ($\xi > 3/16$) This is the case studied in Ye *et al.* [27]. The square root is imaginary in Eq.(7), turning the exponential term into an oscillator. The field will go through damped oscillation around the minimum of V_{eff} at $\phi \simeq 0$ and finally stay there, reproducing GR where the non-minimal coupling effect is negligible.
- **Scaling solution** ($\xi < 3/16$) Both the \pm modes of the MD solution are decaying in this case, but the “−” mode decays faster than the “+” mode and quickly becomes negligible compared with the latter. Therefore it is sufficient to only consider the “+” mode. In this scenario the field adopts a scaling relation $\phi \sim \phi_{\text{ini}} a^{-\gamma}$, $0 < \gamma < 3/4$ and never reaches the minimum of V_{eff} during MD.

In the DE dominating era, the field evolution depends on $V(\phi)$ and cannot be described in general. Fig.2 demonstrates the field evolution in both of the dynamical scenarios.

Lagrangian (1) of TG is not Chameleon screened. However, as Eq.1 is only an EFT of some yet unknown UV-complete gravitational theory on the cosmological scale, it cannot be naively applied to small non-cosmological scales, because new operators will become important when one goes beyond the EFT cutoff energy. In fact, TG (1) can be made properly screened and passing the state-of-the-art experimental constraints on MG by considering only one additional higher order EFT term, see Appendix.A. Therefore, the rest of the paper assumes that TG is properly screened, i.e. it does not violate any local tests of gravity. In particular, this ensures that TG does not impact the micro physics of Cepheids or SNIa [40–43] so one can consistently constrain TG with SNIa data as well as use the SH0ES calibration.

III. DATA AND METHODOLOGY

This paper considers the following datasets:

Cosmological (Λ CDM) Parameters		Model Parameters	
$\Omega_b h^2$	$\mathcal{U}[0.020, 0.025]$	$w_{0,DE}$	$\mathcal{U}[-3, 1]$
$\Omega_c h^2$	$\mathcal{U}[0.1, 0.15]$	$w_{a,DE}$	$\mathcal{U}[-3, 2]$
H_0	$\mathcal{U}[60, 80]$	$\log_{10} \xi$	$\mathcal{U}[-4, 1]$
$\ln 10^{10} A_s$	$\mathcal{U}[3.0, 3.1]$	$\log_{10} \Omega_0$	$\mathcal{U}[-3, -0.5]$
n_s	$\mathcal{U}[0.9, 1.1]$	$\log_{10} \alpha$	$\mathcal{U}[-2, 2]$
τ	$\mathcal{U}[0.04, 0.1]$	$\ln(1 + z_c)$	$\mathcal{U}[7, 10]$
		f_{ede}	$\mathcal{U}[10^{-4}, 0.3]$
		Θ_{ini}	$\mathcal{U}[10^{-2}, 3.1]$

TABLE I. Uniform priors for all cosmological and model parameters.

- **CMB:** The CamSpec version of Planck PR4 high- ℓ TTTEEE [44] data; Planck 2018 low- ℓ TTEE [7] data; CMB lensing of Planck PR4 [45].
- **BAO:** The DESI DR1 BAO measurement [10].
- **SNIa:** Light curve observations of 1550 type Ia Supernovae (SNIa) compiled in the Pantheon+ sample [11], with a single nuisance parameter M_b , the absolute magnitude calibration of SNIa.
- **H_0 :** SNIa absolute magnitude calibration by Cepheids in the host galaxies of 42 SNIa from the SH0ES group [6].
- **LSS:** Galaxy weak lensing (shear) measurement from DES Y1 [46].

The baseline dataset consists of CMB+BAO+SNIa. Since non-linear correction is not yet well-understood in TG, for LSS I use the shear only measurement from DES Y1 with its conservative scale cuts, which does not depend on galaxy bias and only requires the linear power spectrum of the Weyl potential. To compute background and linear cosmology the latest developer version of EFTCAMB [47, 48] is used, based on the Einstein-Boltzmann solver CAMB [49]. Due to the highly non-Gaussian nature of the TG parameter posteriors, the nested sampler PolyChordLite [50, 51] interfaced with Cobaya [52, 53], is used to derive the posteriors. Bayes evidence is computed from the nested sampling output using `anesthetic` [54]. All data and likelihoods used are publicly available with Cobaya.

All models considered have a common set of cosmological parameters, namely the cold dark matter and baryon density, $\omega_c = \Omega_c h^2$ and $\omega_b = \Omega_b h^2$; the Hubble constant H_0 ; the amplitude A_s and spectrum index n_s of the primordial curvature perturbations; and the effective optical depth τ of the reionization process. Current photon temperature is fixed to the measured value $T_{\text{CMB}} = 2.7255$ K [55, 56]. Following Planck [7], neutrino is modeled as two massless and one massive ($m_\nu = 0.06$ eV) reproducing $N_{\text{eff}} = 3.044$ [57–59] and initial temperature $T_\nu = (4/11)^{1/3} T_{\text{CMB}}$. The standard Λ CDM and $w_0 w_a$ CDM model are included in the analysis as reference. In the latter DE is modeled as a fluid with the CPL equation of state $w_{\text{DE}}(a) = w_0 + w_a(1 - a)$ [60, 61] with its perturbations described in the post-Friedmann framework [62].

As explained in section-II, TG also naturally realizes EDE and solves the Hubble tension. Therefore the original axion-like EDE model [31] is also included for comparison. The model has three new parameters, namely the redshift position z_c and height f_{ede} of the EDE energy fraction peak and the EDE field initial position Θ_{ini} , see [31] for details.

Besides the cosmological parameters, TG introduces three new model parameters, the non-minimal coupling ξ , the scalar field initial value ϕ_{ini} and the DE potential parameter λ . Ye *et al.* [27] assumes the GR attractor case ($\xi > 3/16$) to fix the field initial value $\phi_{\text{ini}} = 0$. For full generality ϕ_{ini} is varied in this paper. By Eq.(7), the scalar field is frozen by the Hubble friction during MD thus one can fix $\dot{\phi}_{\text{ini}} = 0$. In practice, the more physically intuitive parameter

$$\Omega_0 = -\xi(\phi_{\text{ini}}/M_p)^2 \quad (8)$$

is sampled in place of ϕ_{ini} . Ω_0 parametrizes the fractional difference in gravity strength between the initial time in RD and today. Similarly, the DE potential parameter λ is also replaced with

$$\alpha = \frac{V_0}{3H_0^2 M_p^2} \lambda^2 e^{-\lambda\phi_{\text{ini}}/M_p} \sim \frac{V_{\phi\phi}(\phi_{\text{ini}})}{R_0}, \quad (9)$$

where R_0 is the curvature today. α characterizes the time when the DE potential $V(\phi)$ dominates over the curvature dependent part in V_{eff} and sources non-minimal coupling (gravity thaws). In particular $\alpha \ll 1$ indicates that $V(\phi)$ never dominates the field evolution until today (gravity never thaws).

Table.I summarizes the priors for all cosmological and model parameters used in this paper. Some beyond Λ CDM models have larger volume of unphysical region near the boundary

	w_0w_a CDM	EDE	TG
Baseline	-1.4	-0.6	+1.5
Baseline+LSS	-1.4	-	+0.5
Baseline+ H_0	+4.6	+9.5	+11.8

TABLE II. Bayes factors $\ln B \equiv \ln Z_{\text{model}} - \ln Z_{\Lambda\text{CDM}}$ compared with ΛCDM for all models studied.

of prior parameter space than ΛCDM , leading to reduced prior volume than ΛCDM and thus potentially bias the Bayes factor *in favor of* the beyond ΛCDM theory. To minimize this effect, priors chosen in Table.I are tighter (but still wide enough to be uninformative) than those typically used in Monte Carlo Markov chain type of analysis.

IV. RESULTS

Table.II summarizes the Bayes factors of w_0w_a CDM, EDE and TG over ΛCDM . TG stands out as the best of all, with moderate evidence over the second best in all of the analysis. Especially, with only the baseline data (CMB+BAO+SNIa), TG is already moderately preferred over ΛCDM and shows moderate and strong evidence over EDE and w_0w_a CDM respectively. This is because TG improves fit to all data, especially the new DESI observation [27]. In baseline+ H_0 , both TG and EDE have very strong evidence over ΛCDM due to the resolution of the Hubble tension, while TG still maintains moderate advantage over EDE with $\ln B = +2.3$. This can be attributed to the fact that TG induces stronger gravity during CMB which negates the need to significantly increase ω_b and ω_c to compensate for the scalar field's impact on CMB [63]. In contrast, such parameter shifts for compensation are ubiquitous in EDE which slightly degrades the CMB fit and causes tension with LSS [38, 64, 65]. Interestingly, according to Appendix.B, the preference for a more scale-invariant primordial curvature spectrum (n_s shifting larger) [65–70] is still present in TG. The state of the cosmological tensions is summarized in Fig.1, which plots the $H_0 - S_8$ posterior distribution for all models in the most constrained baseline+ H_0 analysis. In the following only the results most relevant to the main topic of this paper are shown, while the detailed posterior results and large plots can be found in Appendix-B.

At first note, a peculiarity of Table.II is that w_0w_a CDM is disfavored over ΛCDM in the baseline analysis, opposite to what DESI has found, i.e. a $\ln B \simeq +0.65$ preference for

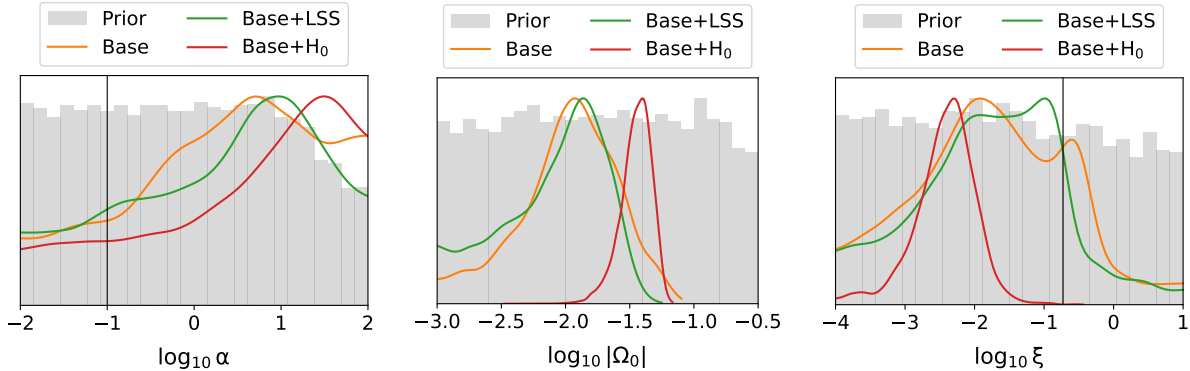


FIG. 3. Comparison of priors (gray histograms) and posterior distributions (lines) of the TG model parameters for the baseline, baseline+LSS and baseline+ H_0 analysis. *Left panel:* the thawing time parameter α defined by Eq.(9). The vertical black line marks $\alpha = 0.1$, left of which gravity does not thaw. *Middle panel:* $\Omega_0 = M_{\text{eff}}^2/M_p^2 - 1$ parametrizes the fractional difference in gravity strength between the initial radiation dominating era and today. *Right panel:* the non-minimal coupling parameter ξ . The vertical black line marks the value $\xi = 3/16$ which separates the GR attractor solutions with the scaling solutions as explained in Section.II.

w_0w_a CDM [10], using also CMB+DESI+PantheonPlus. This might be attributed to the different CMB data (Planck PR4 v.s. PR3), prior choices (as explained in Section.III) and codes (CAMB v.s. CLASS) used ².

According to the discussion about Eq.(9) in Section.II, one could use $\alpha > 0.1$ as a rough criteria for whether gravity thaws or not during DE dominance. Fig.3 compares the prior of α with its posterior, showing that signs of thawing is recovered by all analysis. Despite of a reduced prior volume in $\alpha > 1$ ³, the posterior distributions of α all display visually clear preference for thawing ($\alpha > 0.1$) in Fig.3, which is quantitatively $> 1\sigma$ according to Appendix-B.

Another interesting finding is that, without any H_0 related data to drive the preference for a non-vanishing ϕ_{ini} , it is found $\Omega_0 \neq 0$ at $\gtrsim 2\sigma$ (defined as the prior lower bound outside of the 2σ posterior range) for both the baseline and baseline+LSS analysis. As depicted in Fig.3, both analysis show a broad peak at $\Omega_0 \sim \mathcal{O}(10^{-2})$, implying a 2σ sign

² I have performed the Λ CDM and w_0w_a CDM analysis with exactly the same prior setting and data as DESI but with CAMB (DESI used CLASS), which still yields w_0w_a CDM disfavored over Λ CDM with $\ln B = -1.6$.

Further investigation is ongoing to identify the origin of this difference.

³ Too large α means very early thawing and ϕ displaces too much away from zero, resulting in a small or even negative G_{eff} that leads to solver crash, thus the smaller prior volume.

of early MG, i.e. gravity being percent level stronger than today, during and before the CMB time in the baseline data. Adding SH0ES calibration to SNIa in baseline+ H_0 , which is expected to prefer a EDE-like energy peak near matter-radiation equality thus a non-zero ϕ_{ini} and $\Omega_0 = \xi(\phi_{\text{ini}}/M_p)^2$ to solve the Hubble tension, the posterior of Ω_0 narrows down to $\Omega_0 = 0.037 \pm 0.009$, compatible with the results without H_0 data and corresponding to a $> 4\sigma$ detection of early MG in TG.

Signs of non-minimal coupling $\xi \neq 0$ has also been recovered from all analysis, which is $> 1\sigma$ for baseline and baseline+LSS and $> 4\sigma$ for baseline+ H_0 . Fig.3 shows that, despite the preference for $\xi \neq 0$, without H_0 related observation the data cannot distinguish between the two dynamical scenarios, GR attractor and scaling, and the posterior distribution of ξ is a broad bi-model plateau with two sub-peaks corresponding to the two cases. Ye *et al.* [27] implicitly imposed a prior lower bound $\xi \gtrsim 0.2$ thus studied only the GR attractor sub-case of TG. Previous exploration of non-minimally coupled EDE also mainly focused on the $\xi \gtrsim 0.1$ part of the parameter space by choosing a uniform prior on ξ [71–74]. In contrast, the analysis presented here has moderate more cover of the small ξ parameter space by sampling in log scale, which surprisingly, reveals the fact that it is the $\xi < 3/16$ scaling scenario that is actually more cosmologically preferred than the $\xi > 3/16$ case. Even in the baseline, one notice that the main sub-peak of the two being that corresponds to the scaling solutions. Adding the Hubble tension data further pins down the dynamics to scaling and excludes the GR attractor scenario at $> 5\sigma$.

V. CONCLUSION

In this paper I assessed the credibility of Thawing Gravity as a cosmological model using CMB, BAO, SNIa and LSS data. While originally proposed to explain the recent DESI observation by Ye *et al.* [27], TG performs surprisingly well in the baseline CMB+BAO+SNIa analysis, showing moderate evidence over Λ CDM with a Bayes factor $\ln B = +1.5$. Meanwhile, TG also offers a natural explanation to the Hubble tension, and is very strongly preferred over Λ CDM with $\ln B = +11.8$ in the baseline+ H_0 analysis, while remaining consistent with LSS thanks to the MG effect.

The baseline TG analysis highlights the possibility of early MG with $\Omega_0 \neq 0$ at 2σ , which effectively parametrizes the fractional difference in gravity strength between the CMB era

and today. Taking the SH0ES calibration of the distance ladder into consideration, the finding is consistent with baseline but has much improved precision, turning the 2σ hint into a $> 4\sigma$ detection of early MG in TG. Further study is ongoing to explore the effect of MG during CMB and even earlier times.

As emphasized in the main text, TG should be viewed as an EFT valid on the cosmological scale and care must be taken when applying it to small scales. Using the explicit example TG_s Appendix-A confirmed that in the weak field regime TG is equivalent to general relativity on small scales when higher order EFT operators negligible on the cosmological scale are taken into account. Note that TG_s can still be properly screened even if the higher order operator becomes relevant at the CMB time, which will be studied in a future work. This paper used the relatively old DES Y1 shear only data to constrain TG due to ambiguity in the non-linear regime. Research is currently ongoing to better understand screening and non-linear growth in TG so that one can confront it with full LSS data (shear and clustering) from current and future surveys. It would also be interesting to consider TG-like EFTs in the strong field regime near compact objects.

ACKNOWLEDGMENTS

GY thanks Alessandra Silvestri, Pedro Ferreira, William Wolf for insightful discussions, and Kushal Lodha for help and discussions about the DESI data pipeline. GY acknowledges the ALICE cluster for computational support. Some results are obtained with the help of `Mathematica` and `xAct` [75]. Some figures make use of `GetDist` [76]. This work is supported by NWO and the Dutch Ministry of Education, Culture and Science (OCW) (grant VI.Vidi.192.069).

Appendix A: Screened Thawing Gravity

For the exponential potential studied in the main text, TG (1) is not screened. This can be seen by writing Eq.(3) in spherical coordinates (assuming static spherical symmetric scalar profile and neglecting metric backreaction)

$$\frac{d^2\phi}{dr^2} + \frac{2}{r} \frac{d\phi}{dr} = -\frac{M_p^2}{2} f' R + V' \simeq -\frac{1}{2} f' \rho_m + V' = V'_{\text{eff}} \quad (\text{A1})$$

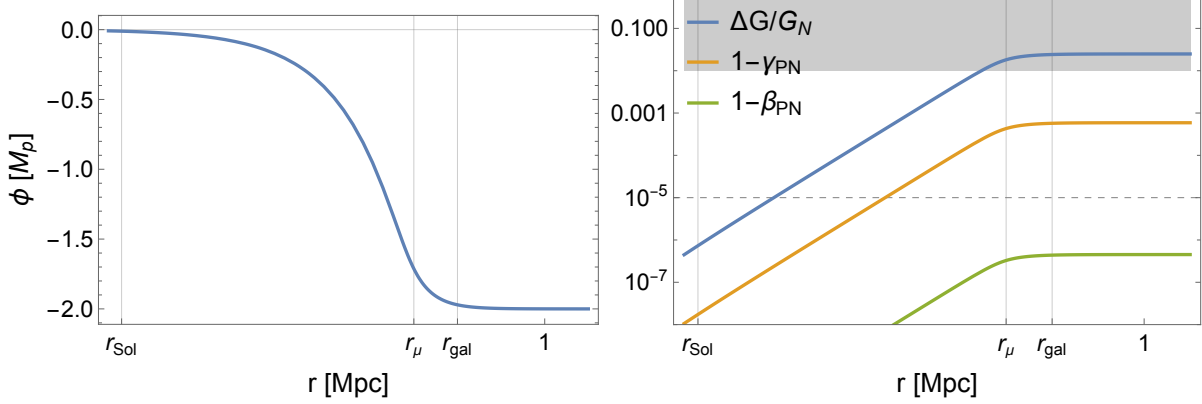


FIG. 4. Screening of the MG effect in TG_s . The scales included are the solar system scale $r_{\text{sol}} \simeq 1.45 \times 10^{-10}$ Mpc, the screening scale $r_\mu = 1$ kpc and the Milky Way scale $r_{\text{gal}} = 8$ kpc. *Left panel:* The radial scalar field profile. *Right panel:* Fractional change in the Newtonian constant $\Delta G/G_N \equiv G_{\text{eff}}/G_N - 1$ and the post-Newtonian parameters γ_{PN} and β_{PN} . Gray shaded region marks a rough estimate of the running in the Newtonian constant that can bias current measurements of the SNIa distance ladder. The dashed gray line marks 10^{-5} , the typical size of current experimental upper bounds on the post-Newtonian parameters [77].

where

$$V_{\text{eff}}(\phi) = \frac{1}{2}\xi\rho_m\phi^2 + V. \quad (\text{A2})$$

To Chameleon screen the MG effect, ϕ must change from its cosmological value to $\phi = 0$ in high density regions. (A1) implies ϕ can only change on a length scale $L_s^{-2} \sim \xi\rho_m/M_p^2$. However, for the Earth with a mean density $\rho \sim 10^3 \text{kg/m}^3$, $L_s \sim \xi^{-1/2}\mathcal{O}(10^8 \text{km})$; for the Milky Way with a mean density of $\rho \sim 0.4 \text{GeV/cm}^3$, $L_R \sim \xi^{-1/2}\mathcal{O}(\text{Mpc})$. With $\xi < 1$ both are much larger than the size of the corresponding object, meaning that the MG effect is unscreened.

However, as argued in the main text, TG should be viewed as an EFT describing gravity on cosmological scales. Concluding TG to be unscreened using Lagrangian (1) is not theoretically consistent because new operators will appear once one goes beyond the EFT cutoff energy. A simple example is the operator $\frac{1}{M_p^2\mu^2}X^2$, which is the next to leading expansion term of the general kinetic operator $P(X)$ that generalizes the canonical kinetic operator X . One could then consider a refined TG EFT Lagrangian

$$\mathcal{L} = \frac{M_p^2}{2} [1 - \xi(\phi/M_p)^2] R + X - \frac{1}{M_p^2\mu^2}X^2 - V_0 \exp(-\lambda\phi/M_p). \quad (\text{A3})$$

Causality ensures the “−” sign before the X^2 operator [78, 79]. This theory will be referred to as screened TG (TG_s). In particular, TG_s will be indistinguishable from TG by BAO, SNIa and LSS if $\mu > \text{Mpc}^{-1}$, and by CMB if $\mu > H(z_{\text{eq}}) \sim 30 \text{ Mpc}^{-1}$.

In TG_s the scalar field equation reads

$$-\left(1 - \frac{2X}{M_p^2 \mu^2}\right) \square \phi - \frac{2}{M_p^2 \mu^2} \phi^\mu \phi_{\mu\nu} \phi^\nu = \frac{M_p^2}{2} f' R - V' \quad (\text{A4})$$

To see the screening explicitly, one can combine the trace of Einstein Eq.(2) with Eq.(A4) to get

$$-\left(1 + \frac{3f'^2 M_p^2}{2f} - \frac{2X}{M_p^2 \mu^2}\right) \square \phi + \frac{3f' f'' M_p^2}{f} X - \frac{2}{M_p^2 \mu^2} \phi^\mu \phi_{\mu\nu} \phi^\nu = -V' - \frac{f'}{2f} (T^{(\phi)} + T^{(m)}). \quad (\text{A5})$$

Assuming spherical symmetry and neglecting the metric back-reaction, Eq.(A5) reduces to an ordinary differential equation with a single variable r . To solve Eq.(A5), let us model the galaxy as a uniform density ball with radius $r_{\text{gal}} = 10 \text{ kpc}$ and filled with pressureless dust $\rho_{\text{gal}} = 8 \text{ GeV/cm}^3 = -T^{(m)}$. Outside of the ball the density is much lower $\rho_{\text{env}} = \rho_{\text{gal}}/1000$. Given the posterior results presented in Appendix.B, the TG parameters are set to $\xi = 0.006$, $\lambda = 1$, $V_0/M_p^2 = 8.4 \times 10^{-8} \text{ Mpc}^{-2} \sim 3\Omega_\Lambda H_0^2$. The screening scale is set to $\mu = 1 \text{ kpc}^{-1}$, which ensures that TG_s is equivalent to TG for all datasets considered in the main text. Use the boundary condition $\phi(r \rightarrow \infty) = -2M_p$ to represent a typical cosmological value of the scalar field and requires standard gravity at small scales, i.e. $\phi(r \rightarrow 0) = 0$, Eq.(A5) is numerically solved with the results plotted in Fig.4. The screening effect is easily visible in the left panel where the field connects between the cosmological value at infinity and the screened value at origin. Moreover, laboratory and solar system experiments usually constrain the effective Newtonian constant G_{eff} and post Newtonian parameters γ_{PN} and β_{PN} . In TG_s they are [80]

$$G_{\text{eff}} = \frac{G_N}{f} \frac{2f + 4f'^2}{2f + 3f'^2}, \quad 1 - \gamma_{\text{PN}} = \frac{f'^2}{f + 2f'^2}, \quad 1 - \beta_{\text{PN}} = \frac{ff'}{4(2f + 3f'^2)} \gamma'_{\text{PN}}. \quad (\text{A6})$$

The right panel of Fig.4 compares the MG parameters of TG_s with existing observational bounds, showing that TG_s is properly screened and passes current experimental tests of gravity. It has been pointed out that G_{eff} running with time might change the SNIa peak luminosity and bias the distance-redshift measurements from SNIa [40–43], with the expected peak luminosity running $L \sim G^\gamma$, $\gamma \sim \mathcal{O}(1)$ and consequently the SNIa absolute magnitude

Parameter	Baseline	Baseline+LSS	Baseline+ H_0
$\log(10^{10} A_s)$	3.044 ± 0.013	3.043 ± 0.013	3.051 ± 0.014
n_s	0.9666 ± 0.0036	0.9673 ± 0.0035	0.9700 ± 0.0035
H_0	67.77 ± 0.35	67.91 ± 0.32	68.43 ± 0.34
$\Omega_b h^2$	0.02227 ± 0.00013	0.02229 ± 0.00012	0.02242 ± 0.00012
$\Omega_c h^2$	0.11854 ± 0.00077	0.11822 ± 0.00074	0.11719 ± 0.00076
τ_{reio}	0.0564 ± 0.0068	$0.0566^{+0.0064}_{-0.0075}$	0.0610 ± 0.0072
M_b	-19.429 ± 0.010	-19.4255 ± 0.0096	$-19.408^{+0.011}_{-0.0096}$
S_8	0.8176 ± 0.0086	0.8140 ± 0.0081	0.8050 ± 0.0085

TABLE III. Mean and 68% posterior constraints of the cosmological parameters in Λ CDM.

variation $\Delta M_b \sim \mathcal{O}(\Delta G(z)/G_N)$. From Appendix.B it can be seen that M_b is constrained with absolute precision ~ 0.01 cosmologically, roughly corresponding to the gray shaded band in the right panel of Fig.4. At the SNIa scale, which is much smaller than r_{sol} , $\Delta G/G_N$ in TG_s is many orders of magnitude below the cosmological data sensitivity. Therefore, using SNIa to constrain TG is justified.

In conclusion, constraining TG with cosmological data, as done in the main text, while assuming proper screening on smaller scales is theoretically consistent and justified. In the above example of TG_s , the adopted screening scale is $\mu = 1 \text{ kpc}^{-1}$ such that TG_s is equivalent to TG also for CMB. However, a smaller μ is also possible and will cause screening to start from even larger scales. Especially, $\mu \sim \mathcal{O}(10 \text{ Mpc}^{-1})$ is particularly interesting because the X^2 operator can now be constrained by CMB observations, and possibly also next-generation LSS [81, 82].

Appendix B: Detailed Posterior Results

This appendix collects the large tables and contour plots of the posterior results for all analysis performed in the main text. The tables and plots are grouped by model, namely Λ CDM (Table.III, Fig.5), $w_0 w_a$ CDM (Table.IV, Fig.6), EDE (Table.V, Fig.7) and TG (Table.VI, Fig.8). For comparison, the baseline Λ CDM is included in all plots.

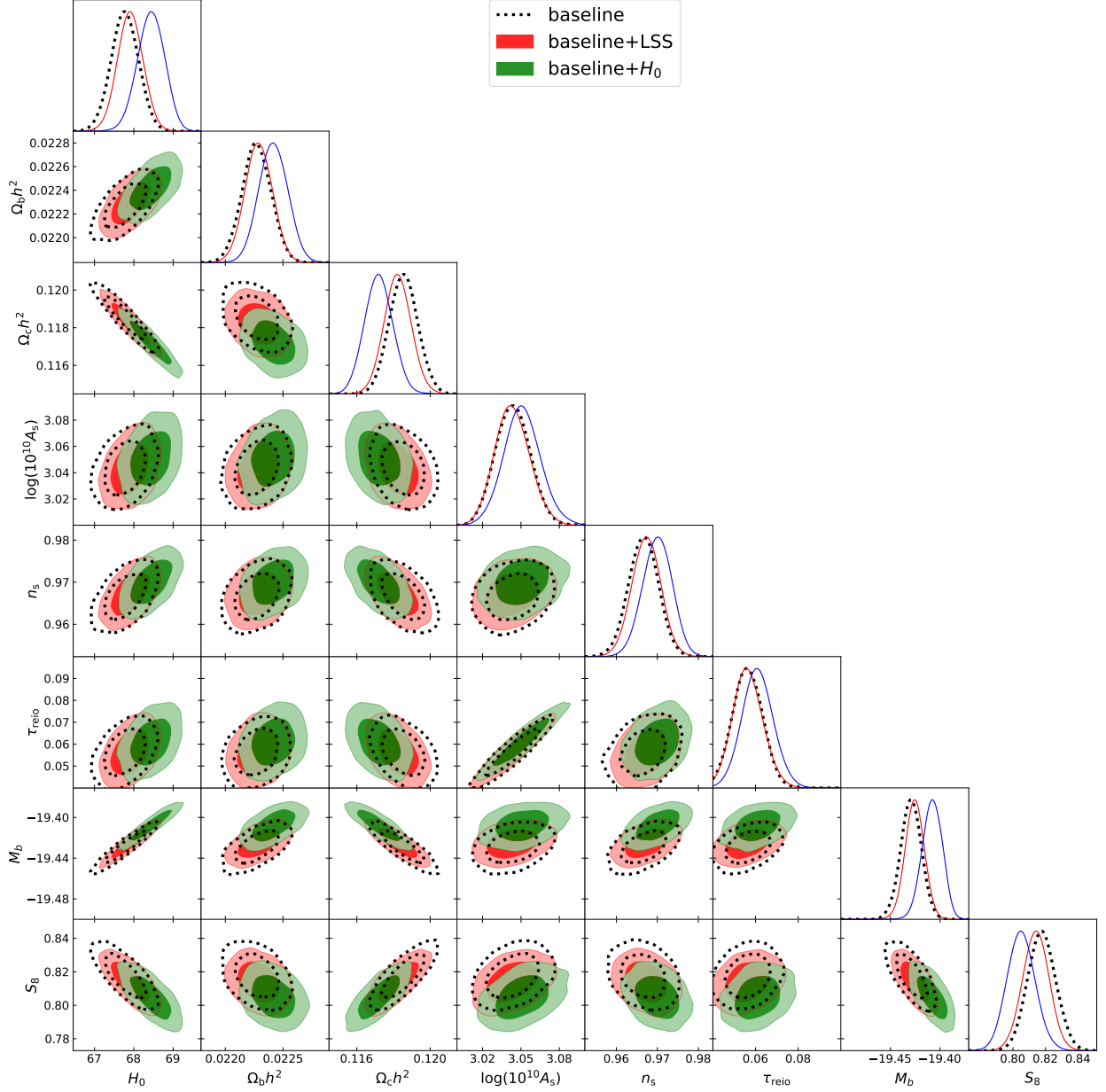


FIG. 5. 68% and 95% posterior distribution of the cosmological parameters in Λ CDM.

-
- [1] L. Perivolaropoulos and F. Skara, *New Astron. Rev.* **95**, 101659 (2022), arXiv:2105.05208 [astro-ph.CO].
 - [2] G. Efstathiou (2024) arXiv:2406.12106 [astro-ph.CO].
 - [3] E. Abdalla *et al.*, *JHEAp* **34**, 49 (2022), arXiv:2203.06142 [astro-ph.CO].
 - [4] A. G. Riess, *Nature Rev. Phys.* **2**, 10 (2019), arXiv:2001.03624 [astro-ph.CO].

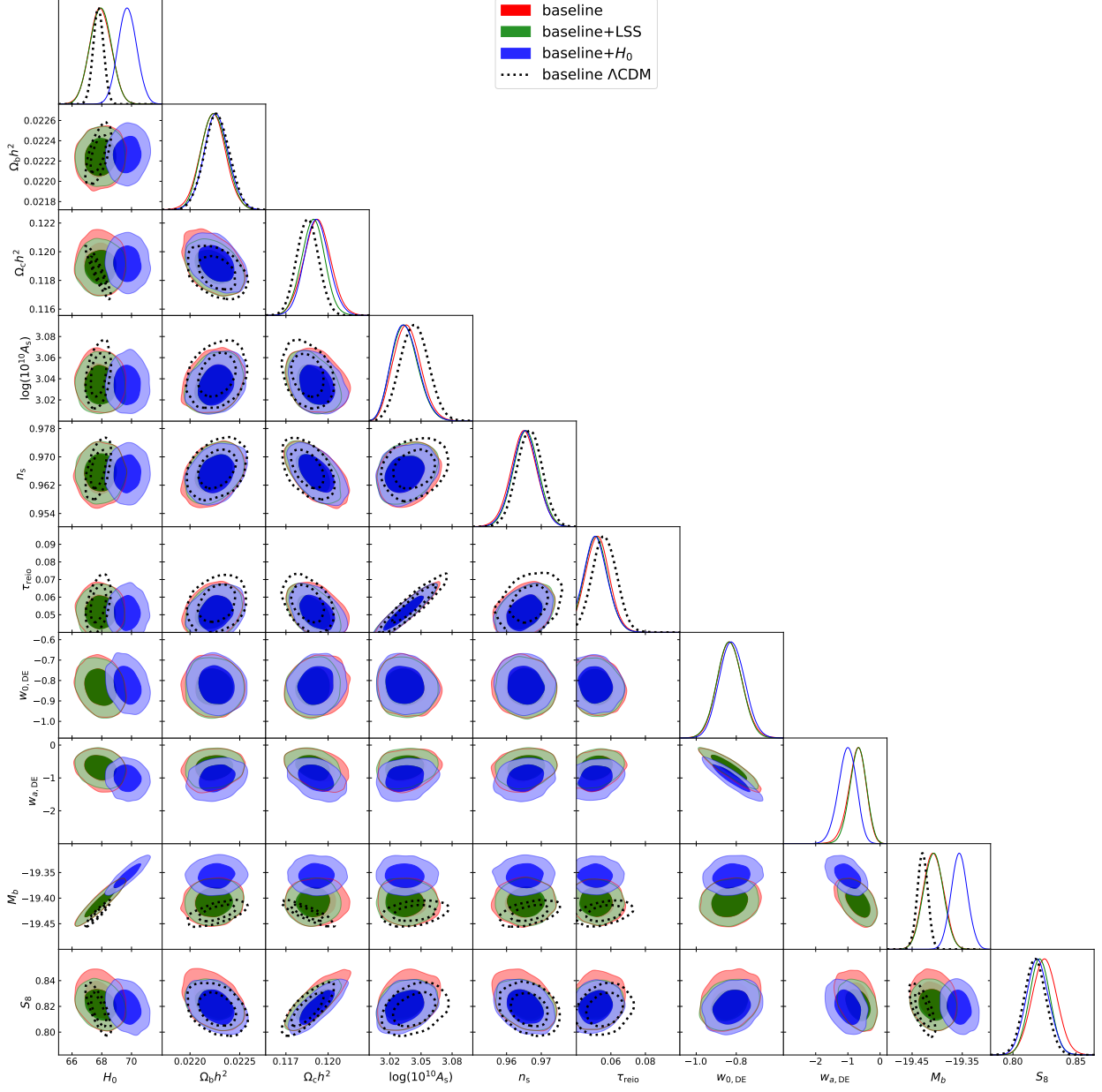


FIG. 6. 68% and 95% posterior distribution of all cosmological and model parameters in $w_0 w_a$ CDM. The baseline Λ CDM is included as reference (dashed lines).

- [5] E. Di Valentino, O. Mena, S. Pan, L. Visinelli, W. Yang, A. Melchiorri, D. F. Mota, A. G. Riess, and J. Silk, *Class. Quant. Grav.* **38**, 153001 (2021), arXiv:2103.01183 [astro-ph.CO].
- [6] A. G. Riess *et al.*, *Astrophys. J. Lett.* **934**, L7 (2022), arXiv:2112.04510 [astro-ph.CO].
- [7] N. Aghanim *et al.* (Planck), *Astron. Astrophys.* **641**, A5 (2020), arXiv:1907.12875 [astro-ph.CO].
- [8] E. Di Valentino *et al.*, *Astropart. Phys.* **131**, 102604 (2021), arXiv:2008.11285 [astro-ph.CO].

Parameter	Baseline	Baseline+LSS	Baseline+ H_0
$\log(10^{10} A_s)$	$3.037^{+0.012}_{-0.014}$	$3.035^{+0.011}_{-0.014}$	$3.035^{+0.011}_{-0.014}$
n_s	0.9650 ± 0.0038	0.9656 ± 0.0036	0.9653 ± 0.0036
H_0	67.91 ± 0.71	67.92 ± 0.71	69.72 ± 0.62
$\Omega_b h^2$	0.02223 ± 0.00013	0.02224 ± 0.00012	0.02226 ± 0.00012
$\Omega_c h^2$	0.11922 ± 0.00094	0.11893 ± 0.00082	0.11919 ± 0.00086
τ_{reio}	$0.0528^{+0.0058}_{-0.0072}$	$0.0521^{+0.0054}_{-0.0072}$	$0.0520^{+0.0054}_{-0.0074}$
$w_{0,\text{DE}}$	-0.831 ± 0.063	-0.834 ± 0.062	-0.821 ± 0.062
$w_{a,\text{DE}}$	$-0.72^{+0.30}_{-0.24}$	$-0.69^{+0.27}_{-0.24}$	$-1.02^{+0.30}_{-0.25}$
M_b	-19.408 ± 0.020	-19.407 ± 0.019	-19.356 ± 0.016
S_8	0.8249 ± 0.0098	0.8212 ± 0.0082	0.8196 ± 0.0089

TABLE IV. Mean and 68% posterior constraints of the cosmological and model parameters in $w_0 w_a$ CDM.

- [9] T. M. C. Abbott *et al.* (Kilo-Degree Survey, DES), *Open J. Astrophys.* **6**, 2305.17173 (2023), arXiv:2305.17173 [astro-ph.CO].
- [10] A. G. Adame *et al.* (DESI), (2024), arXiv:2404.03002 [astro-ph.CO].
- [11] D. Scolnic *et al.*, *Astrophys. J.* **938**, 113 (2022), arXiv:2112.03863 [astro-ph.CO].
- [12] D. Rubin *et al.*, (2023), arXiv:2311.12098 [astro-ph.CO].
- [13] T. M. C. Abbott *et al.* (DES), *Astrophys. J. Lett.* **973**, L14 (2024), arXiv:2401.02929 [astro-ph.CO].
- [14] B. R. Dinda, (2024), arXiv:2405.06618 [astro-ph.CO].
- [15] M. Cortês and A. R. Liddle, (2024), arXiv:2404.08056 [astro-ph.CO].
- [16] V. Patel and L. Amendola, (2024), arXiv:2407.06586 [astro-ph.CO].
- [17] G. Liu, Y. Wang, and W. Zhao, (2024), arXiv:2407.04385 [astro-ph.CO].
- [18] G. Efstathiou, (2024), arXiv:2408.07175 [astro-ph.CO].
- [19] D. Wang, (2024), arXiv:2404.13833 [astro-ph.CO].
- [20] Y. Carloni, O. Luongo, and M. Muccino, (2024), arXiv:2404.12068 [astro-ph.CO].
- [21] E. O. Colgáin, M. G. Dainotti, S. Capozziello, S. Pourojaghi, M. M. Sheikh-Jabbari, and D. Stojkovic, (2024), arXiv:2404.08633 [astro-ph.CO].
- [22] O. Luongo and M. Muccino, (2024), arXiv:2404.07070 [astro-ph.CO].

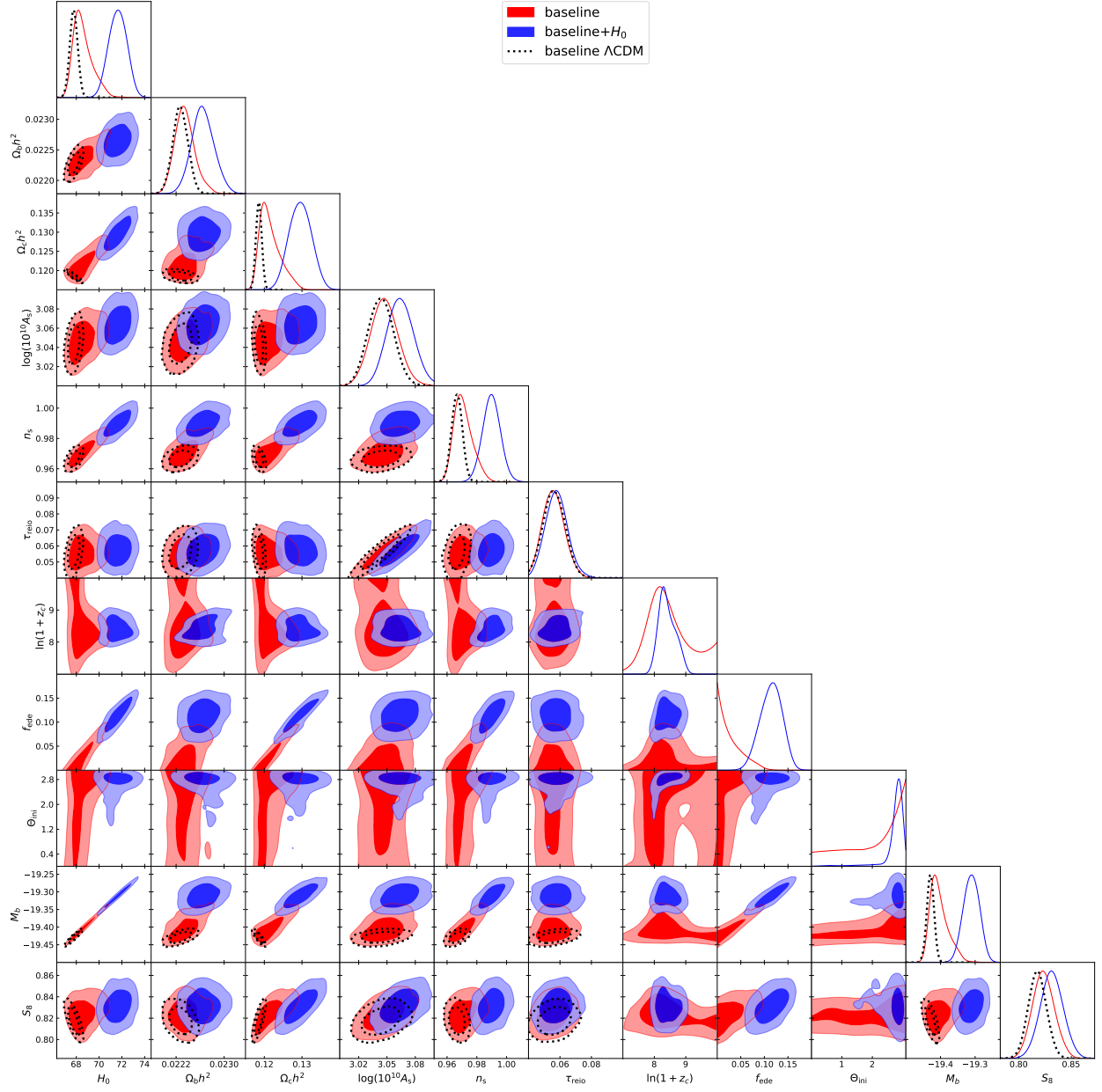


FIG. 7. 68% and 95% posterior distribution of the cosmological and model parameters in EDE. The baseline Λ CDM is included as reference (dashed lines).

[23] Z. Huang *et al.*, (2024), arXiv:2405.03983 [astro-ph.CO].

[24] X. D. Jia, J. P. Hu, and F. Y. Wang, (2024), arXiv:2406.02019 [astro-ph.CO].

[25] Z. Wang, S. Lin, Z. Ding, and B. Hu, (2024), arXiv:2405.02168 [astro-ph.CO].

[26] D. Shlivko and P. J. Steinhardt, Phys. Lett. B **855**, 138826 (2024), arXiv:2405.03933 [astro-ph.CO].

[27] G. Ye, M. Martinelli, B. Hu, and A. Silvestri, (2024), arXiv:2407.15832 [astro-ph.CO].

Parameter	Baseline	Baseline+ H_0
$\log(10^{10} A_s)$	3.047 ± 0.014	3.064 ± 0.014
n_s	$0.9708^{+0.0046}_{-0.0074}$	0.9898 ± 0.0060
H_0	$68.56^{+0.49}_{-1.0}$	71.64 ± 0.78
$\Omega_b h^2$	$0.02234^{+0.00014}_{-0.00018}$	0.02265 ± 0.00019
$\Omega_c h^2$	$0.1215^{+0.0014}_{-0.0034}$	0.1296 ± 0.0029
τ_{reio}	$0.0560^{+0.0061}_{-0.0075}$	0.0579 ± 0.0070
$\ln(1 + z_c)$	$8.46^{+0.45}_{-0.74}$	$8.41^{+0.25}_{-0.29}$
f_{ede}	< 0.0362	$0.114^{+0.025}_{-0.022}$
Θ_{ini}	> 1.61	$2.75^{+0.19}_{+0.016}$
M_b	$-19.405^{+0.015}_{-0.031}$	-19.311 ± 0.023
S_8	0.823 ± 0.010	0.831 ± 0.011

TABLE V. Mean and 68% posterior constraints of the cosmological and model parameters in EDE.

- [28] W. J. Wolf, P. G. Ferreira, and C. García-García, (2024), arXiv:2409.17019 [astro-ph.CO].
- [29] H. Jeffreys, *The Theory of Probability*, Oxford Classic Texts in the Physical Sciences (1939).
- [30] T. Karwal and M. Kamionkowski, Phys. Rev. D **94**, 103523 (2016), arXiv:1608.01309 [astro-ph.CO].
- [31] V. Poulin, T. L. Smith, T. Karwal, and M. Kamionkowski, Phys. Rev. Lett. **122**, 221301 (2019), arXiv:1811.04083 [astro-ph.CO].
- [32] F. Niedermann and M. S. Sloth, Phys. Rev. D **103**, L041303 (2021), arXiv:1910.10739 [astro-ph.CO].
- [33] P. Agrawal, F.-Y. Cyr-Racine, D. Pinner, and L. Randall, Phys. Dark Univ. **42**, 101347 (2023), arXiv:1904.01016 [astro-ph.CO].
- [34] M.-X. Lin, G. Benevento, W. Hu, and M. Raveri, Phys. Rev. D **100**, 063542 (2019), arXiv:1905.12618 [astro-ph.CO].
- [35] G. Ye and Y.-S. Piao, Phys. Rev. D **101**, 083507 (2020), arXiv:2001.02451 [astro-ph.CO].
- [36] M. Kamionkowski and A. G. Riess, Ann. Rev. Nucl. Part. Sci. **73**, 153 (2023), arXiv:2211.04492 [astro-ph.CO].
- [37] V. Poulin, T. L. Smith, and T. Karwal, Phys. Dark Univ. **42**, 101348 (2023), arXiv:2302.09032 [astro-ph.CO].

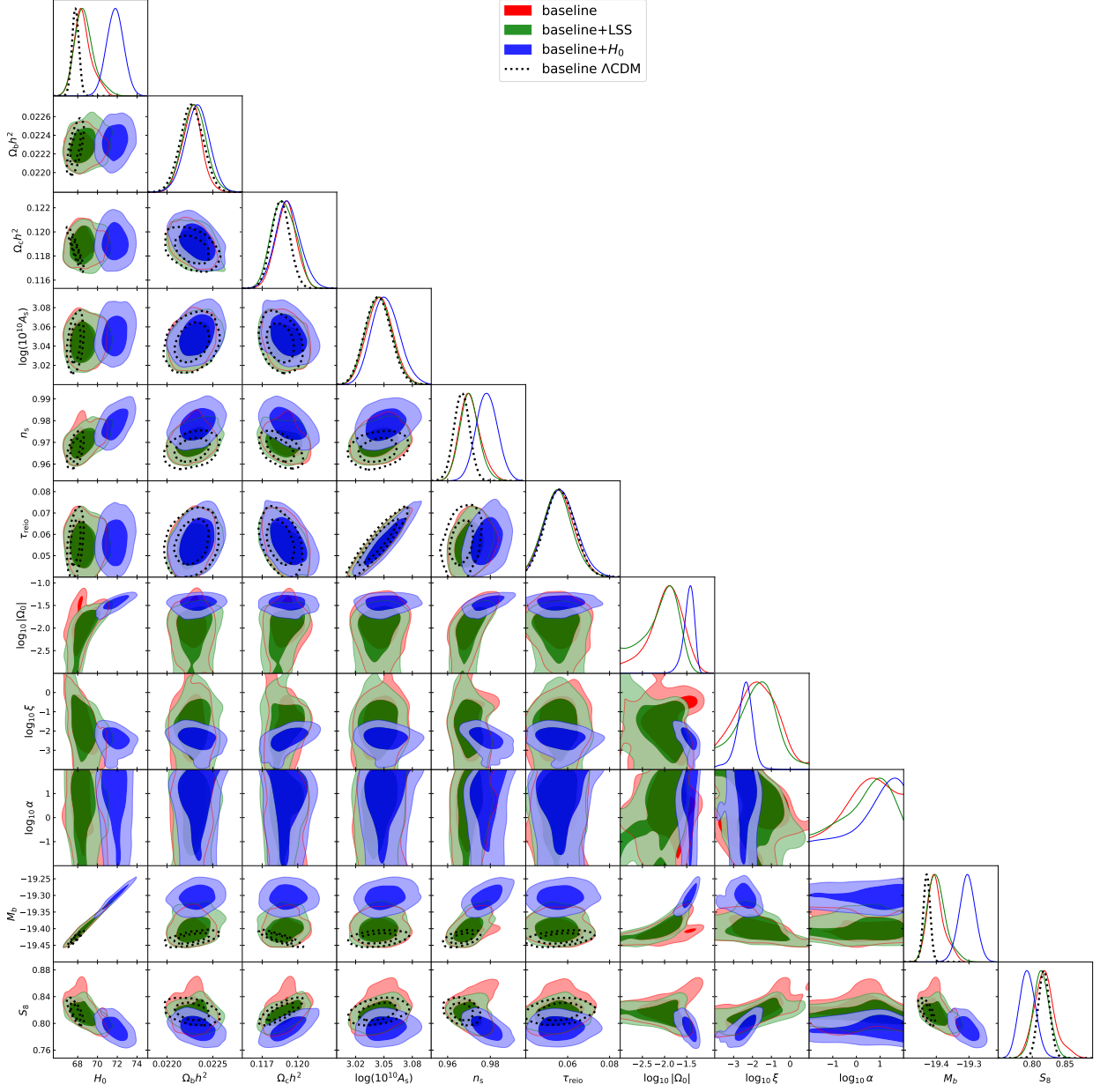


FIG. 8. 68% and 95% posterior distribution of the cosmological and model parameters in TG. The baseline Λ CDM is included as reference (dashed lines).

- [38] J. C. Hill, E. McDonough, M. W. Toomey, and S. Alexander, *Phys. Rev. D* **102**, 043507 (2020), arXiv:2003.07355 [astro-ph.CO].
- [39] T. Damour and K. Nordtvedt, *Phys. Rev. Lett.* **70**, 2217 (1993).
- [40] E. Garcia-Berro, E. Gaztanaga, J. Isern, O. Benvenuto, and L. Althaus, (1999), arXiv:astro-ph/9907440.
- [41] A. Riazuelo and J.-P. Uzan, *Phys. Rev. D* **66**, 023525 (2002), arXiv:astro-ph/0107386.

Parameter	Baseline	Baseline+LSS	Baseline+ H_0
$\log(10^{10} A_s)$	3.046 ± 0.014	3.044 ± 0.014	$3.052^{+0.014}_{-0.015}$
n_s	$0.9705^{+0.0041}_{-0.0054}$	$0.9702^{+0.0041}_{-0.0047}$	0.9784 ± 0.0050
H_0	$68.53^{+0.64}_{-1.0}$	$68.67^{+0.75}_{-1.1}$	71.78 ± 0.86
$\Omega_b h^2$	0.02227 ± 0.00011	0.02230 ± 0.00013	0.02233 ± 0.00013
$\Omega_c h^2$	0.11900 ± 0.00087	$0.11881^{+0.00095}_{-0.0011}$	0.1192 ± 0.0010
τ_{reio}	$0.0559^{+0.0066}_{-0.0076}$	$0.0555^{+0.0064}_{-0.0073}$	$0.0569^{+0.0068}_{-0.0080}$
$\log_{10} \Omega_0 $	$-1.96^{+0.44}_{-0.28}$	$-2.09^{+0.51}_{-0.23}$	$-1.45^{+0.14}_{-0.085}$
$\log_{10} \xi$	$-1.78^{+1.4}_{-0.86}$	$-1.76^{+1.1}_{-0.81}$	$-2.42^{+0.45}_{-0.32}$
$\log_{10} \alpha$	> -0.143	$0.29^{+1.6}_{-0.62}$	> 0.138
M_b	$-19.401^{+0.018}_{-0.030}$	$-19.398^{+0.021}_{-0.032}$	-19.305 ± 0.025
S_8	$0.819^{+0.013}_{-0.017}$	0.814 ± 0.012	0.793 ± 0.012

TABLE VI. Mean and 68% posterior constraints of the cosmological and model parameters in TG.

- [42] S. Nesseris and L. Perivolaropoulos, Phys. Rev. D **73**, 103511 (2006), arXiv:astro-ph/0602053.
- [43] B. S. Wright and B. Li, Phys. Rev. D **97**, 083505 (2018), arXiv:1710.07018 [astro-ph.CO].
- [44] E. Rosenberg, S. Gratton, and G. Efstathiou, Mon. Not. Roy. Astron. Soc. **517**, 4620 (2022), arXiv:2205.10869 [astro-ph.CO].
- [45] J. Carron, M. Mirmelstein, and A. Lewis, JCAP **09**, 039 (2022), arXiv:2206.07773 [astro-ph.CO].
- [46] T. M. C. Abbott *et al.* (DES), Phys. Rev. D **98**, 043526 (2018), arXiv:1708.01530 [astro-ph.CO].
- [47] B. Hu, M. Raveri, N. Frusciante, and A. Silvestri, Phys. Rev. D **89**, 103530 (2014), arXiv:1312.5742 [astro-ph.CO].
- [48] M. Raveri, B. Hu, N. Frusciante, and A. Silvestri, Phys. Rev. D **90**, 043513 (2014), arXiv:1405.1022 [astro-ph.CO].
- [49] A. Lewis, A. Challinor, and A. Lasenby, Astrophys. J. **538**, 473 (2000), arXiv:astro-ph/9911177 [astro-ph].
- [50] W. J. Handley, M. P. Hobson, and A. N. Lasenby, Mon. Not. Roy. Astron. Soc. **450**, L61 (2015), arXiv:1502.01856 [astro-ph.CO].

- [51] W. J. Handley, M. P. Hobson, and A. N. Lasenby, *Mon. Not. Roy. Astron. Soc.* **453**, 4385 (2015), arXiv:1506.00171 [astro-ph.IM].
- [52] J. Torrado and A. Lewis, *JCAP* **05**, 057 (2021), arXiv:2005.05290 [astro-ph.IM].
- [53] J. Torrado and A. Lewis, “Cobaya: Bayesian analysis in cosmology,” *Astrophysics Source Code Library*, record ascl:1910.019 (2019).
- [54] W. Handley, *J. Open Source Softw.* **4**, 1414 (2019), arXiv:1905.04768 [astro-ph.IM].
- [55] D. J. Fixsen, E. S. Cheng, J. M. Gales, J. C. Mather, R. A. Shafer, and E. L. Wright, *Astrophys. J.* **473**, 576 (1996), arXiv:astro-ph/9605054.
- [56] D. J. Fixsen, *Astrophys. J.* **707**, 916 (2009), arXiv:0911.1955 [astro-ph.CO].
- [57] J. J. Bennett, G. Buldgen, P. F. De Salas, M. Drewes, S. Gariazzo, S. Pastor, and Y. Y. Y. Wong, *JCAP* **04**, 073 (2021), arXiv:2012.02726 [hep-ph].
- [58] J. Froustey, C. Pitrou, and M. C. Volpe, *JCAP* **12**, 015 (2020), arXiv:2008.01074 [hep-ph].
- [59] K. Akita and M. Yamaguchi, *JCAP* **08**, 012 (2020), arXiv:2005.07047 [hep-ph].
- [60] M. Chevallier and D. Polarski, *Int. J. Mod. Phys. D* **10**, 213 (2001), arXiv:gr-qc/0009008.
- [61] E. V. Linder, *Phys. Rev. Lett.* **90**, 091301 (2003), arXiv:astro-ph/0208512.
- [62] W. Hu and I. Sawicki, *Phys. Rev. D* **76**, 104043 (2007), arXiv:0708.1190 [astro-ph].
- [63] G. Ye and A. Silvestri, (2024), arXiv:2407.02471 [astro-ph.CO].
- [64] G. Ye and Y.-S. Piao, *Phys. Rev. D* **102**, 083523 (2020), arXiv:2008.10832 [astro-ph.CO].
- [65] G. Ye, B. Hu, and Y.-S. Piao, *Phys. Rev. D* **104**, 063510 (2021), arXiv:2103.09729 [astro-ph.CO].
- [66] G. Ye, J.-Q. Jiang, and Y.-S. Piao, *Phys. Rev. D* **106**, 103528 (2022), arXiv:2205.02478 [astro-ph.CO].
- [67] J.-Q. Jiang, G. Ye, and Y.-S. Piao, *Mon. Not. Roy. Astron. Soc.* **527**, L54 (2023), arXiv:2210.06125 [astro-ph.CO].
- [68] J.-Q. Jiang and Y.-S. Piao, *Phys. Rev. D* **105**, 103514 (2022), arXiv:2202.13379 [astro-ph.CO].
- [69] J.-Q. Jiang, G. Ye, and Y.-S. Piao, *Phys. Lett. B* **851**, 138588 (2024), arXiv:2303.12345 [astro-ph.CO].
- [70] H. Wang, G. Ye, J.-Q. Jiang, and Y.-S. Piao, (2024), arXiv:2409.17879 [astro-ph.CO].
- [71] M. Braglia, M. Ballardini, F. Finelli, and K. Koyama, *Phys. Rev. D* **103**, 043528 (2021), arXiv:2011.12934 [astro-ph.CO].

- [72] M. Braglia, M. Ballardini, W. T. Emond, F. Finelli, A. E. Gumrukecuoglu, K. Koyama, and D. Paoletti, *Phys. Rev. D* **102**, 023529 (2020), arXiv:2004.11161 [astro-ph.CO].
- [73] T. Adi and E. D. Kovetz, *Phys. Rev. D* **103**, 023530 (2021), arXiv:2011.13853 [astro-ph.CO].
- [74] G. Franco Abellán, M. Braglia, M. Ballardini, F. Finelli, and V. Poulin, *JCAP* **12**, 017 (2023), arXiv:2308.12345 [astro-ph.CO].
- [75] J. M. Martin-Garcia, “xAct: Efficient tensor computer algebra for the Wolfram Language,” .
- [76] A. Lewis, (2019), arXiv:1910.13970 [astro-ph.IM].
- [77] C. M. Will, *Living Rev. Rel.* **17**, 4 (2014), arXiv:1403.7377 [gr-qc].
- [78] A. Adams, N. Arkani-Hamed, S. Dubovsky, A. Nicolis, and R. Rattazzi, *JHEP* **10**, 014 (2006), arXiv:hep-th/0602178.
- [79] V. Chandrasekaran, G. N. Remmen, and A. Shahbazi-Moghaddam, *JHEP* **11**, 015 (2018), arXiv:1804.03153 [hep-th].
- [80] B. Boisseau, G. Esposito-Farese, D. Polarski, and A. A. Starobinsky, *Phys. Rev. Lett.* **85**, 2236 (2000), arXiv:gr-qc/0001066.
- [81] Y. Mellier *et al.* (Euclid), (2024), arXiv:2405.13491 [astro-ph.CO].
- [82] R. Mandelbaum *et al.* (LSST Dark Energy Science), arXiv e-prints (2018), arXiv:1809.01669 [astro-ph.CO].